Neck instability of bright solitons in normally dispersive Kerr media

Simon-Pierre Gorza[1,*], Bernard Deconinck[2], Thomas Trogdon[2], Philippe Emplit[1], and Marc Haelterman[1]

[1] *Service OPERA-photonique, Université libre de Bruxelles (ULB), 50 Avenue F. D. Roosevelt, CP194/5 B-1050 Bruxelles, Belgium.*

[2] *Department of Applied Mathematics, University of Washington Campus Box 352420, Seattle, WA, 98195, USA.*

[*] *Corresponding author: sgorza@ulb.ac.be*

Compiled September 28, 2012

The neck instability of bright solitons of the hyperbolic nonlinear Shrödinger equation is investigated. It is shown that this instability originates from a four-wave mixing interaction that links on-axis to off-axis radiation at opposite frequency bands. Our experiment supports this interpretation.

OCIS codes: 190.3100, 190.4420, 190.6135, 190.4380.

Symmetry-breaking instability of solitons has been studied in different areas of physics and appears as a common feature shared by most solitons despite the diversity of the physical systems that support them [1–3]. In optics, the break-up of self guided light beams through transverse and/or modulational instability has been demonstrated for solitons in self-focussing and defocusing Kerr media [1, 4] as well as in second harmonic generation media [5]. In particular, for the case of focusing Kerr nonlinearity, the dynamics is governed by the nonlinear Schrödinger (NLS) equation that possesses solutions in the form of bright (1+1)D spatial solitons. When propagating in a (2+1)D media, these solitons are known to be unstable against periodic perturbations in the extra transverse dimension in which they are uniform (regardless of the relative sign between the dispersion (diffraction) terms, i.e. in both elliptic and hyperbolic systems) [6, 7]. In hyperbolic systems, such as normally dispersive planar waveguides, the transverse instability in (2+1)D leads to a spontaneous breaking of spatial bright soliton stripe into a spatiotemporal snake like pattern. However, beside the well known snake instability branch in the cubic soliton spectrum, another instability branch associated with a neck type instability has recently been identified theoretically [8] and experimentally [9]. Neck instability of spatially localized waves has also been reported in other media with normal dispersion, such as bulk media [10], coupled nonlinear waveguides [11] or quadratic media [12]. However, this neck instability is counterintuitive since it is well known that continuous waves are stable when propagating in a (1+1)D normally dispersive focusing Kerr medium. This is the reason why we propose in the present Letter a detailed theoretical and experimental analysis of the neck instability of solitons of the (2+1)D hyperbolic NLS equation. As we shall see, this instability shares some properties with light filament dynamics that occur in spatially localized beams propagating in normally dispersive bulk media [13].

Let us consider the hyperbolic nonlinear Schrödinger equation with normal time dispersion:

$$i\frac{\partial\psi}{\partial Z}+\frac{1}{2}\frac{\partial^2\psi}{\partial X^2}-\frac{1}{2}\frac{\partial^2\psi}{\partial T^2}+|\psi|^2\psi=0. \tag{1}$$

In optics, this equation describes the dynamics of the slowly varying spatiotemporal envelope of the electric field $E = A_0\psi\exp(ik_0z - i\omega_0t)$, of carrier frequency ω_0 and propagation constant k_0. In this equation, $Z = z/L_{\mathrm{NL}}$, $X = x(L_{\mathrm{NL}}/k_0)^{-1/2}$ and $T = (t - zv_g^{-1})(L_{\mathrm{NL}}k_0'')^{-1/2}$ are the normalized longitudinal, transverse and time coordinates, respectively, and $L_{\mathrm{NL}} = 1/(\gamma A_0^2)$ is the nonlinear length, where γ is the nonlinear coefficient of the waveguide; k_0'' is the group velocity dispersion coefficient and $v_g = 1/k_0'$ is the group velocity of light in the waveguide.

The fundamental bright soliton stripe solution of Eq.1 is $\psi = \mathrm{sech}(X)\exp(iZ/2)$. The stability analysis has shown that this solution is unstable against perturbations of the form [8]:

$$p_\Gamma(X;\Omega) = \epsilon_0(u+iv)\exp(iZ/2), \tag{2}$$

with $\{u, v\} = [\{U(X), V(X)\}\exp(i\Omega T + \Gamma Z) + c.c.]$, where the eigenfunctions $\{U, V\}$ are complex functions of the transverse coordinate X; Ω is the modulation frequency and *c.c.* denotes the complex conjugate of the previous term. Mathematically, U and V are solutions of the the linear eigenvalue problem resulting from the linearization of the equation of motion obtained by injecting the perturbed solution $\psi = \mathrm{sech}(x) + p_\Gamma$ into (1) [8]. Note that if the perturbation p_Γ, given by (U, V, Γ, Ω), is unstable with the gain g then $p^*_{\Gamma^*}$ described by $(U^*, V^*, \Gamma^*, \Omega)$ is also unstable with the same gain but opposite drift velocity. These two solutions represent two physically discernible solutions and are generally distinct, meaning that p_Γ and $p^*_{\Gamma^*}$ may grow independently depending on how the instability is seeded. Fig.1(a), shows the instability gain ($g = 2\mathrm{Re}[\Gamma]$) as a function of Ω for the neck and the snake instability (i.e. for even and odd U and V, respectively). As can be seen, as far as the neck instability is concerned, temporal modulations are neutrally stable for small Ω. For frequencies

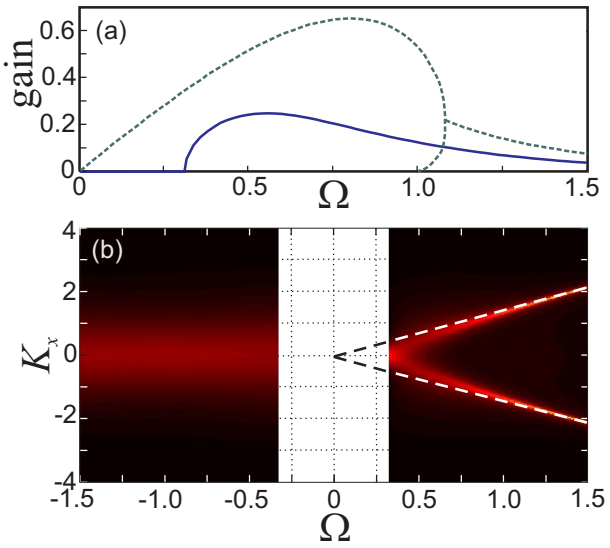

Fig. 1. (color online) (a) Neck (solid curve) and snake (dashed curve) instability gain. (b) Density plot of $|\tilde{p}_\Gamma|$ as a function of the frequency detuning Ω. The amplitude has been normalized so that the energy $\int_{-\infty}^{\infty} |\tilde{p}_\Gamma|^2 dK_x$ is independent of Ω in each sidebands. The dashed lines show the relation $K_x = \pm\sqrt{2}\Omega$ for $\Omega > 0$.

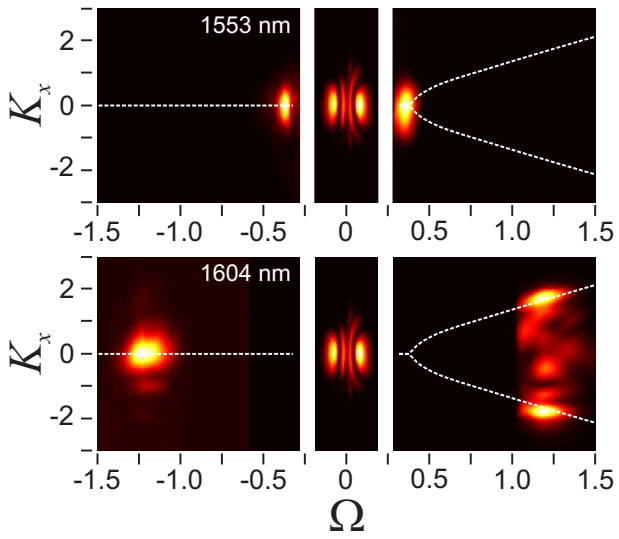

Fig. 2. (color online) Measured spatiotemporal spectrum at the output of a 5 mm long waveguide when a soliton beam (center panels) is launched together with a seed beam with a negative frequency detuning close (top) and far (bottom) from the threshold. The peak power at the waveguide input are 1,3 kW and $\sim$ 140 mW, respectively. The intensity has been normalized to one in each panel for revealing the structure of the spectrum in the sidebands. The white dotted curve shows the theoretical dominant transverse frequency of $\tilde{p}_\Gamma$.

larger than the frequency threshold $\Omega_t \approx 0.31$, the eigenmodes are unstable as a result of a Hamiltonian Hopf bifurcation similarly to the one reported in the context of modulational instability of quadratic solitons [12]. Moreover, the neck instability exhibits no high frequency cutoff contrary to the neck instability of bright solitons in anomalous dispersive media [7].

The neck instability of bright solitons of the (2+1)D NLS equation may be understood as a noncollinear four-wave mixing interaction driven by Kerr nonlinearity, similarly to the Y-shaped instability of spatially localized nonlinear mode occurring in normally dispersive bulk media [13]. Indeed, for transversally localized waves, efficient amplification of new frequencies is possible when one of the two sideband waves is noncollinear with the soliton beam. Let us assume that the signal wave (with frequency $\omega_0 - \Delta\omega$) is collinear with the soliton beam (with the propagation constant k^s and k^p respectively) and let $k_\perp^i$ be the transverse projection of the wave vector of the idler wave (with frequency $\omega_0 + \Delta\omega$ and propagation constant k^i). It can be shown that the nonlinear longitudinal phase matching condition ($k_z^s + k_z^i = 2k_z^p$) leads to the power independent relation $k_\perp^i = \pm(2k_0 k_0^{"})^{1/2}\Delta\omega$ when cross phase modulation on the idler wave is assumed to be negligible owing to the transversally confined character of the soliton beam. In dimensionless variables this later dispersion relation becomes $K_\perp^i = \pm\sqrt{2}\Omega$. This simple analysis suggests that the angularly resolved spectrum of the neck instability has off-axis transverse components.

In order to confirm this interpretation, the two dimensional Fourier transform (with respect to T and X) $\tilde{p}_\Gamma(K_x;\Omega)$ of the symmetric unstable eigenmodes was computed for frequency detunig Ω larger than Ω_t. The spatially symmetric eigenfunctions U and V of Eq. 2 were obtained by numerically solving the linear eigenvalue problem. As can be seen in Fig. 1(b), $|\tilde{p}_\Gamma|$ features a single peak centered on $K_x = 0$ in the negative frequency sideband of the spatiotemporal spectrum. In the positive sideband, this spectrum is composed of a single peak for frequencies close to Ω_t but of two narrow peaks for large frequency detunings. As the frequency detuning increases, the position of the maxima become closer to the theoretical curve $K_x = \pm\sqrt{2}\Omega$ (see dashed lines in Fig.1) which supports the interpretation of this neck instability as a noncollinear wave-mixing interaction.

These results were investigated both numerically and experimentally. We performed numerical simulations of the propagation, according to Eq.1, of a perturbed soliton beam of the form $\mathrm{sech}(X) * (1 + \epsilon\exp[i\Omega T])$. The simulations show that after few nonlinear lengths of propagation, the spatiotemporal spectrum in the signal and idler sideband clearly feature one or two main peaks whose position agree with the theoretical results reported in Fig.1. Moreover, the finite time duration of the soliton beam does not prevent the neck instability to grow as long as it is significantly longer than the characteristic time of the modulation ($2\pi/\Omega$).

In the experiment, the neck instability of optical bright solitons was studied in normally dispersive planar waveguides made up of semiconductor AlGaAs alloys. The experimental setup is similar to that of Ref. [14]. Because of the limited size and resolution of the InGaAs camera,

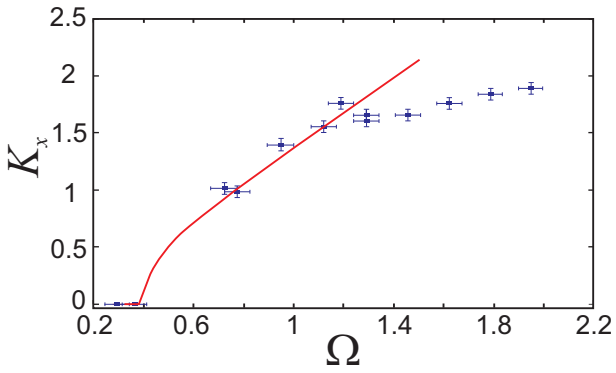

Fig. 3. (color online) Transverse wavenumber of the peaks in the idler sideband as a function of the frequency detuning Ω. The theoretical red curve shows the dominant transverse frequency of $\tilde{p}_\Gamma$. The length of the horizontal and vertical bars correspond to the spectral width of the seed beam (6 nm) and to the camera resolution, respectively.

the whole angularily resolved spectra was recorded in three separate measurements to cover 250 nm. The central wavelength of the soliton beam was set to 1536 nm while the seed beam could continuously be tuned from $\sim$ 1500 nm to $\sim$ 1650 nm. The soliton and the seed beams had the same input profile and a width of 17 μm. Despite the higher snake gain, we can experimentally favor the development of the neck instability, thanks to the opposite parity between the neck and the snake unstable modes. In order to maximize the initial amplitude of the unstable mode of the neck instability, the seed beam is set collinear with the soliton beam with no lateral shift. This also prevents the snake instability to be efficiently seeded because of the central node in the spatial profile of its unstable modes. In the experiment, the two instabilities were distinguished through their characteristic signature in the spatiotemporal spectrum. Moreover, the temporal modulation at the waveguide input strongly breaks the symmetry along the Ω axis. We thus expect to observe mainly the growth of p_Γ which is characterized by axial downshifted frequencies emission. ${p^*}_{\Gamma^*}$ has indeed a weak overlap with the actual seed beam since its spectrum is a reflection of the spectrum of p_Γ about $\Omega = 0$. Fig.2 shows typical results of two-dimensional spectra recorded at the waveguide output. As can be seen, at a seed wavelength of 1553 nm, both the signal and the idler waves have their angular spectrum localized around the zero traverse frequency, in agreement with the theoretical results for small frequency detunings (see white dashed line). For larger detunigs, the spectra clearly show a double peak structure on the idler side and a single peak structure on the signal side. This therefore demonstrate that for large detuning the amplification of on axis downshifted frequencies is accompanied by the generation of upshifted angularly off-axis frequencies.

The dependence of the transverse wavenumber of the maxima in the idler sideband with the seed beam frequency detuning is reported in Fig. 3 and compared with the theoretical results of Fig. 1(b). In the experiment, it was clearly observed that the transverse wavenumber of the idler waves increases with the modulation frequency Ω past a given threshold. As can be seen, there is a very good agreement between theory and the experimental results up to $\Omega \approx 1.2$. For larger Ω values, it appears that the transverse wavenumber of the two maxima in the idler sideband is lower than expected from theory and numerical simulations. This discrepancy between theory and experiment remains unclear and is not related to the imaging systems nor to linear and nonlinear propagation losses in the waveguide in accordance with the power independent dispersion relation. Note that for such large detunings, a qualitative difference between the neck and the snake instability spectra in the idler sideband can still be observed since the peaks of the neck instability have always a larger transverse wavenumber than those of the snake instability. Previous experiments on the snake instability have also featured a similar discrepancy between theoretical and experimental spectra for large detunings [14].

In conclusion, by means of a spatiotemporal spectral analysis of light propagation in a semiconductor planar waveguide we have demonstrated experimentally that the neck instability of the bright solitons of the hyperbolic nonlinear Schrodinger equation relies on noncollinear phase-matched four-wave mixing processes. Our experimental observations are in excellent agreement with the linear stability analysis of the bright soliton as well as with a simple geometrical approach of the phase-matching condition.

This work was supported by the Belgian Science Policy Office under Grant No. IAP-VI10 and by the Fonds de la Recherche Fondamentale Collective, Grant No. 2.4513.06.

References

1. A. V. Mamaev et al., Phys. Rev. A **54,** 870 (1996).
2. Z. Dutton et al., Science **293,** 663 (2001).
3. N. R. Pereira, A. Sen, and A. Bers, Phys. Fluids **21,** 117 (1978).
4. S.-P. Gorza et al., Phys. Rev. Lett. **92,** 084101 (2004).
5. X. Liu, K. Beckwitt, and F. Wise, Phys. Rev. Lett. **85,** 1871 (2000).
6. V. E. Zakharov and A. M. Rubenchik, Sov. Phys. JETP **38,** 494 (1974).
7. Y. S. Kivshar and D. E. Pelinovsky, Phys. Report **331,** 117 (2000).
8. B. Deconinck et al., Proc. Roy. Soc. A **462,** 2039 (2005).
9. S.-P. Gorza et al., Phys. Rev. Lett. **102,** 134101 (2009).
10. K. Germaschewski et al., Physica D **151,** 175 (2001).
11. A.V. Yulin et al., Opt. exp. **14,** 12347 (2006).
12. D. V. Skryabin, Phys. Rev. E **60,** 7511 (1999).
13. M. A. Porras et al., Phys. Rev. A **76,** (2007), 011803.
14. S.-P. Gorza et al., Phys. Rev. Lett. **106,** 094101 (2011).

References

1. A. V. Mamaev, M. Saffman, D. Z. Anderson, and A. A. Zozulia, "Propagation of light beams in anisotropic nonlinear media: From symmetry breaking to spatial turbulence," Phys. Rev. A **54,** 870 (1996).
2. Z. Dutton, M. Budde, C. Slowe, and L. V. Hau, "Observation of Quantum Shock Waves Created with Ultra-Compressed Slow Light Pulses in a Bose-Einstein Condensate," Science **293,** 663 (2001).
3. N. R. Pereira, A. Sen, and A. Bers, "Nonlinear development of lower hybrid cones," Phys. Fluids **21,** 117 (1978).
4. S.-P. Gorza, N. Roig, Ph. Emplit, and M. Haelterman, "Snake Instability of a Spatiotemporal Bright Soliton Stripe," Phys. Rev. Lett. **92,** 084101 (2004).
5. X. Liu, K. Beckwitt, and F. Wise, "Transverse Instability of Optical Spatiotemporal Solitons in Quadratic Media," Phys. Rev. Lett. **85,** 1871 (2000).
6. V. E. Zakharov and A. M. Rubenchik, 'Ìnstability of waveguides and solitons in nonlinear media," Sov. Phys. JETP **38,** 494 (1974).
7. Y. S. Kivshar and D. E. Pelinovsky, "SELF-FOCUSING AND TRANSVERSE INSTABILITIES OF SOLITARY WAVES," Phys. Report **331,** 117 (2000).
8. B. Deconinck, D. E. Pelinovsky, and J. D. Carter, "Transverse instabilities of deep-water solitary waves", Proc. Roy. Soc. A **462,** 2039 (2005).
9. S.-P. Gorza, P. Kockaert, Ph. Emplit, and M. Haelterman, "Oscillatory Neck Instability of Spatial Bright Solitons in Hyperbolic Systems," Phys. Rev. Lett. **102,** 134101 (2009).
10. K. Germaschewski, R. Grauer, L. Bergé, V.K. Mezentsev, and J.J. Raasmussen, "Splittings, coalescence, bunch and snake patterns in the 3D nonlinear Schrödinger equation with anisotropic dispersion," Physica D **151,** 175 (2001).
11. A.V. Yulin, D.V. Skryabin, and A.G. Vladimirov, "Modulational instability of discrete solitons in coupled waveguides with group velocity dispersion," Opt. exp. **14,** 12347 (2006).
12. D. V. Skryabin, "Role of internal and continuum modes in modulational instability of quadratic solitons," Phys. Rev. E **60,** 7511 (1999).
13. M. A. Porras et al., "Light-filament dynamics and the spatiotemporal instability of the Townes profile," Phys. Rev. A **76,** (2007), 011803.
14. S.-P. Gorza, B. Deconinck, Ph. Emplit, T. Trogdon, and M. Haelterman, "Experimental Demonstration of the Oscillatory Snake Instability of the Bright Soliton of the (2+1)D Hyperbolic Nonlinear Schro ?dinger Equation," Phys. Rev. Lett. **106,** 094101 (2011).